Development/Plasticity/Repair

Long-Term Potentiation in the Juvenile Superior Colliculus Requires Simultaneous Activation of NMDA Receptors and L-type Ca^{2+} Channels and Reflects Addition of Newly Functional Synapses

Jian-Ping Zhao, Marnie A. Phillips, and Martha Constantine-Paton
The McGovern Institute for Brain Research, Massachusetts Institute of Technology, Cambridge, Massachusetts 02139

The visual layers of the rodent superficial superior colliculus (sSC) have been the focus of many development studies of the molecular bases of retinotopic map formation, the role of early retinal waves in this process, and the development of glutamate synapses. Previous studies have documented long-term potentiation (LTP), believed to be critical to developmental synapse refinement, in the rodent sSC. However, the means of induction and the preparations used have varied widely, and thus cellular changes underlying this LTP remain ambiguous. Whole-cell and perforated patch clamping were used in this study to elucidate the cellular mechanism of electrically evoked LTP in the juvenile rat sSC. This LTP required relatively low-frequency stimulation (20 Hz) and simultaneous activation of NMDA receptors and L-type Ca^{2+} channels. Experiments focused on narrow-field vertical neurons, a documented excitatory cell type in the stratum griseum superficiale using bipolar stimulation in the stratum opticum. Strontium (Sr^{2+}) replacement of calcium (Ca^{2+}) was applied to study evoked quantal events before and after LTP induction at the same synapses. Paired-pulse ratio and coefficient of variance analyses examined presynaptic release. Increases in quantal frequency were invariably found in the absence of increases in quantal amplitude and probability of release. These data suggest that electrically stimulated LTP, in the juvenile sSC after eye opening, selectively involves the addition or stabilization of AMPA receptors at the large number of silent synapses known to appear in the sSC after eye opening.

Key words: **LTP; NMDA receptors; L-type Ca^{2+} channels; silent synapses; quantal frequency; probability of release**

Introduction

NMDA receptor (NMDAR)-dependent long-term potentiation (LTP) is an intensively studied form of plasticity, and much work has focused on the CA3-to-CA1 principal neuron synapse in the hippocampus. At this synapse *in vitro*, LTP is dependent on Ca^{2+} influx through NMDAR and/or L-type Ca^{2+} channels (Grover and Teyler, 1990; Moosmang et al., 2005) and is associated with an increase in quantal size and frequency of the AMPA receptor (AMPAR) response as well as with increases in the probability of transmitter release and/or active synapses (Bekkers and Stevens, 1990; Malinow and Tsien, 1990; Liao et al., 1995; Oliet et al., 1996; Isaac et al., 1997; Nicoll, 2003).

NMDAR-dependent LTP is particularly important to studies of synapse development and stabilization. NMDARs are the first ionotropic receptors detected at glutamate synapses, and NMDAR function is critical to the activity-dependent insertion or removal of AMPARs underlying synapse refinement (Constantine-Paton, 1990; Constantine-Paton and Cline, 1998). Stabilizing AMPARs in synapses ("unsilencing" synapses) by high-frequency excitation that drives NMDARs is a mechanism underlying LTP prominently encountered when ingrowing afferents begin activity-dependent refinement (Durand et al., 1996; Wu et al., 1996; Poncer, 2003; Groc et al., 2006).

In this study, we use a slice preparation encompassing the visual layers of the rat superficial superior colliculus (sSC) and focus on a specific excitatory neuron cell type with whole-cell and perforated patch-clamp recording to elucidate sSC LTP. Previous studies have verified field potential LTP in the sSC, but a wide variety of expression mechanisms have been reported (Miyamoto et al., 1990; Hirai and Okada, 1993; Miyamoto and Okada, 1993; Platt and Withington, 1998; Platt et al., 1998; Lo and Mize, 2002). The rodent sSC has been used extensively for studies of the developmental determinants of glutamate neurotransmission (Lu and Constantine-Paton, 2004; van Zundert et al., 2004), the role of retinal waves (Torborg and Feller, 2005), and Eph–Ephrin interactions in retinocollicular map formation (McLaughlin and O'Leary, 2005). NMDAR function is known to be critical for the later stages of retinocollicular map refinement (Simon et al., 1992). A cellular understanding of NMDAR-dependent LTP in the sSC would help to advance mechanistic understanding (Dalva et al., 2000) in such studies.

Received Aug. 23, 2006; revised Oct. 23, 2006; accepted Oct. 30, 2006.

This work was supported by National Institutes of Health Grant EY014074 (M.C.-P.). We thank H. R. Horvitz for helpful comments on this manuscript.

Correspondence should be addressed to Jian-Ping Zhao, Massachusetts Institute of Technology, 77 Massachusetts Avenue, Building 46-4165, Cambridge, MA 02139. E-mail: jpzhao@mit.edu.

DOI:10.1523/JNEUROSCI.3678-06.2006

 0270-6474/06/2612647-09$15.00/0

In rats and mice, pattern vision begins to instruct visual pathway development, and corticocollicular afferents refine during the third postnatal week (Inoue et al., 1992; Goldberg and Constantine-Paton, 2005) to attain registration with the previously formed retinocollicular map (Simon and O'Leary, 1992). Here we report that *in vitro* LTP in the postnatal day 15 (P15) to P17 sSC, unlike CA1 LTP, requires simultaneous NMDAR and L-type Ca^{2+} channel activity and involves only the formation of new functional synapses, probably by AMPAR addition, to the large number of silent synapses present during this period after eye opening (Lu and Constantine-Paton, 2004).

Materials and Methods

Animals. Rat pups were obtained from Charles River Laboratories (Wilmington, MA) and maintained with their mothers in Massachusetts Institute of Technology (MIT) facilities under the supervision of the Department of Comparative Medicine. All maintenance and procedures concerning these animals were in accordance with approved MIT Animal Care and Use Committee protocols.

Slice preparation. SC slices were prepared as described previously (Colonnese et al., 2005). P15–P17 Sprague Dawley rats (day of birth counted as P0) were anesthetized with isoflurane and decapitated. The midbrain was dissected and placed in ice-cold artificial CSF (ACSF) containing the following (in mM): 124 NaCl, 3 $MgCl_2$, 4 KCl, 3 $CaCl_2$, 1.25 $NaHPO_4$, 26 $NaHCO_3$, and 16 D-glucose saturated with 95% O_2/5% CO_2 to a final pH of 7.35. Parasagittal slices (350 μm thick) were cut in ice-cold ACSF with a vibratome (1000-plus sectioning system) and incubated in ACSF for at least 1 h at 32–34°C before recording. During the experiments, individual slices were transferred to a submersion-type recording chamber in which they were continuously superfused at 3–4 ml/min with ACSF or with ACSF in which 3 mM Sr^{2+} was substituted for 3 mM Ca^{2+} (Sr^{2+}ACSF). Slices for LTP experiments were maintained at temperatures of 32–33°C, whereas others were maintained at room temperature (22–24°C).

Bicuculline methiodide (12 μM, a $GABA_A$ receptor antagonist; Sigma, St. Louis, MO) was present in all experiments. D-2-Amino-5-phosphonopentanoic acid (AP-5; 50–100 μM, an NMDAR antagonist; Sigma), 6,7-dinitroquinoxaline-2,3-dione (DNQX; 10 μM, a selective non-NMDAR antagonist; Sigma), 1,4-dihydro-2,6-dimethyl-4-(3-nitrophenyl)-3,5-pyridinedicarboxylic acid 2-methyloxyethyl 1-methylethyl ester (nimodipine, 20 μM, an L-type Ca^{2+} channel antagonist; Tocris, Ellisville, MO), and tetrodotoxin (TTX) (1 μM, a voltage-dependent Na^+ channel antagonist; Sigma) were added to bath solutions in different experiments.

Electrophysiological protocol. Whole-cell and perforated patch-clamp recordings were made from selected neurons in stratum griseum superficiale (SGS) of the P15–P17 rat SC slices. The selected neurons lie in the intermediate and deeper SGS and have radially elongated or pyramidal cell bodies with several apical and basal dendrites directed, respectively, toward the pia and the deeper collicular layers. These cells have been termed narrow-field vertical neurons by previous investigators (Langer and Lund, 1974) and have been shown to be excited by visual stimulation in rodents (Mooney et al., 1985) and to be glutamatergic in cats (Jeon et al., 1997). Neuronal soma and proximal dendrites were visualized using a Nikon (Tokyo, Japan; E600FN) infrared differential interference contrast (DIC) microscope with a 60× water-immersion objective and video camera (CCD-300T-RC; DAGE MTI, Michigan City, IN) and filled with biocytin (see below) in 15–20 experiments to verify the relationship between the DIC images and the full extent of the dendritic arbor.

Recording pipettes with 4–6 MΩ resistance were pulled from borosilicate glass (outer diameter, 1.2 mm; inner diameter, 0.69 mm) by a P-97 pipette puller (Sutter Instruments, Novato, CA). These pipettes were for both whole-cell and perforated patch-clamp recordings.

The pipette solution for whole-cell recording contained the following (in mM): 105 K-gluconate, 30 KCl, 10 phosphocreatine, 10 HEPES, 4 ATP-Mg, 0.3 GTP, 0.2 EGTA, and 0.5% biocytin (w/v; Sigma), pH adjusted to 7.3 with KOH and osmolarity adjusted to ~298 mmol/kg with sucrose. When BAPTA (10 mM; Sigma) was used, EGTA was omitted in the pipette solution; when the perforated patch-clamp recording was performed, the pipette tip was filled with the above-mentioned pipette solution and backfilled with the same pipette solution containing amphotericin B (400 μg/ml; Sigma).

Series resistance in whole-cell recording experiments were monitored by injection of hyperpolarizing current pulses (100 pA, 50 ms) when using current-clamp configuration or by negative voltage steps (−2 mV, 30 ms) when using voltage-clamp configuration. Input resistances were always <40 MΩ, and if any input resistance changed ±20%, the data were eliminated from additional analysis. Cells were held at −70 mV in the Mg^{2+}-containing ACSF for all recordings in voltage clamp.

Electrical signals were amplified with an Axopatch 200B amplifier, digitized with a Digidata 1322A interface (Molecular Devises, Union City, CA), filtered at 2 kHz, sampled at 10 kHz, and stored in a Pentium III computer that provided on-line response display and off-line data analysis. pClamp 8.1 (Molecular Devices) and Mini version 6.0 (Synaptosoft, Decatur, GA) were used to acquire and analyze data. All averages are listed as means ± SEM unless otherwise stated. The statistical criterion for significance was $*p < 0.05$ and $**p < 0.01$.

Stimulation. To evoke synaptic responses from the selected neurons in SGS, constant current stimuli at pulse durations from 0.2 to 0.3 ms were delivered through a bipolar tungsten stimulating electrode (tip separations between 50 and 100 μm) placed in the stratum opticum (SO), the major afferent pathway to the sSC. Stimulation intensity was adjusted from 1/3 to ~1/2 of the threshold for eliciting action potentials and maintained at that level throughout the recordings for test and tetanic stimuli. LTP was induced by a single 20-s-long burst of 20 Hz current. We specifically avoided use of a pairing protocol in this work because previous studies in the sSC revealed a large component of extrasynaptic NMDARs in the young colliculus (Townsend et al., 2003), and we wanted to maximize Ca^{2+} influx at the postsynaptic density (PSD) in this study.

LTP protocol. In the LTP experiments, EPSPs or EPSCs were assayed with test stimuli delivered at 0.05 Hz over at least 10 min of stable recording before and 35 min after the inducing stimulation. In the initial experiments (see Results), a range of potential LTP-inducing stimuli was applied, and the optimal "inducing" stimulus for the SO-to-SGS pathway was determined to be 400 pulses at 20 Hz for 20 s. As a measure of synaptic strength, the initial slope of the EPSPs from ~10 to 60% of the rising phase or amplitude of EPSCs was measured. To generate summary graphs, the slope of each test EPSP or amplitude of each test EPSC in an experiment was first normalized to the average slope or amplitude value over a 10 min baseline period. The average response graphs for a group of experiments with the same treatment were subsequently obtained by calculating the average and SE of the values for each time point in the experiments across all experiments in the group. To determine whether there was a long-term change in synaptic strength after application of the inducing stimulus, the mean EPSP slope or EPSC amplitude during the baseline was compared with the mean EPSP slope or EPSC amplitude during an interval 25–35 min after "induction" using a paired-sample *t* test (Grover and Teyler, 1990; Lo and Mize, 2002). To statistically compare results across treatment groups, the mean normalized EPSP slopes during 25–35 min after induction were compared using a nonparametric Kruskal–Wallis test with a Steel–Dwass multiple comparison procedure.

Determination of quantal changes. Sr^{2+}-induced asynchronous synaptic responses were acquired in voltage-clamp mode by delivery of stimuli at 0.1 Hz. Amplitudes and frequencies of the asynchronous events were measured during a 400 ms period beginning 30 ms after stimulus. This approach eliminated the initial synchronous synaptic responses. Amplitude values of the miniature currents from an individual experiment were normalized to the average amplitude and averaged across the experiments in each treatment group. Data for amplitude and inter-event interval collected before and after LTP induction were compared using the nonparametric Kolmogorov–Smirnov test.

Assays for presynaptic change. To test for a change in the probability of glutamate release before and after LTP induction, test stimuli were given as pairs, separated by a 50 ms interval. Using this protocol, the evoked EPSC2 amplitude/EPSP1 amplitude ratio was quantified to obtain a paired-pulse ratio (PPR) for each 0.05 Hz test stimulus. The mean PPR during 10 min baseline before LTP induction was compared with that during the 25–35 min interval after LTP induction using a paired *t* test.

The coefficient of variation (CV) was calculated as CV = SD/M, where M is the mean. SD and M are calculated from 30 successively evoked EPSC1s during 10 min of baseline recording before and between 25 and 35 min after LTP induction.

Biocytin labeling. After electrophysiological recording sessions, slices with biocytin-loaded neurons were processed as described previously (Hughes et al., 2000). Briefly, slices were fixed overnight in 4% paraformaldehyde in 0.1 M phosphate buffer (PB), pH 7.2, at 4°C, washed in PB, and incubated in PB-based cytoprotectant solutions as follows: twice for 10 min in 10% sucrose (w/v), twice for 10 min in 20% sucrose with 6% glycerol, and twice for 30 min in 30% sucrose and 12% glycerol; they were then placed in envelopes of aluminum foil, frozen and thawed three times, washed in PB and then in 0.1 M PBS, incubated in Texas Red Avidin D (diluted 1:250 in PBS; Vector Laboratories, Burlingame, CA), and again washed in PBS. Sections were mounted on glass slides in 50% glycerol in PBS and coverslipped. Labeled neurons in these slices were imaged with a confocal microscope (PCM 2000; Nikon) controlled by the Compix (Cranberry Township, PA) software package running on a Pentium-based personal computer.

Results

Stimulation at 20 Hz for 20 s induces LTP

LTP of the field potential has been demonstrated in sSC recordings (Okada, 1993; Platt and Withington, 1998; Lo and Mize, 2002). Consequently, we first evaluated whether similar LTP could be obtained by whole-cell recording from single neurons. To minimize variation in results attributable to neuron type, we focused recording on narrow-field vertical neurons (Langer and Lund, 1974) believed to be prominent excitatory neurons in the SGS (Fig. 1*A*) (Mooney et al., 1985; Jeon et al., 1997). These neurons express L-type Ca^{2+} channels in the mouse sSC (Mize et al., 2002) and probably correspond to the vertical fusiform neurons thought to be glutamate-containing relay cells in the cat's SC (Jeon et al., 1997).

EPSPs were evoked at SO-to-SGS synapses by delivering stimuli to the SO at 0.05 Hz before and after a potential LTP-inducing stimulation was applied. Representative LTP data from one cell exposed to the optimal inducing stimulus, 20 Hz for 20 s, is shown in Figure 1*B*. The averaged data from all 15 neurons exposed to this inducing stimulus is illustrated in Figure 1*C*. The enhanced synaptic responses persisted for as long as stable recordings were maintained. The mean EPSP slope measured between 25 and 35 min after induction was 124.3 ± 6.2% of the control value observed 10 min before the inducing stimulation ($n = 15$; $p < 0.01$) (Fig. 1*C*).

In these experiments, stimulus strength was chosen so that a postsynaptic action potential response was rare (see Materials and Methods). Nevertheless, the induction of LTP in the sSC was exceptionally sensitive to the frequency and/or number of applied pulses. We fixed the duration of stimulation at 20 s, a duration used previously for sSC LTP induction (Lo and Mize, 2002), and varied frequency from 10 to 50 Hz. As can be seen in Figure 2*A*, only pulses at 20 Hz produced a significant LTP in the SGS neurons when averaged across all of the cells examined using this induction frequency. In contrast, 50 Hz stimulation for 20 s produced a significant long-term depression (LTD). One contribution to this frequency selectivity is likely to be fatigue in the afferents as the poststimulus depression became more pronounced between stimulation at 40 and 50 Hz (Fig. 2*E*,*F*). Other active responses in the sSC dendrites such as I_h, I_a K^+, or even the L-type Ca^{2+} channel activity itself (Magee, 2000; Watanabe et al., 2002; Wang et al., 2003) could be the basis of the frequency tuning in the 10–30 Hz range (Fig. 2*B–D*) and perhaps the tendency toward depression late in the 40 or 50 Hz responses as well.

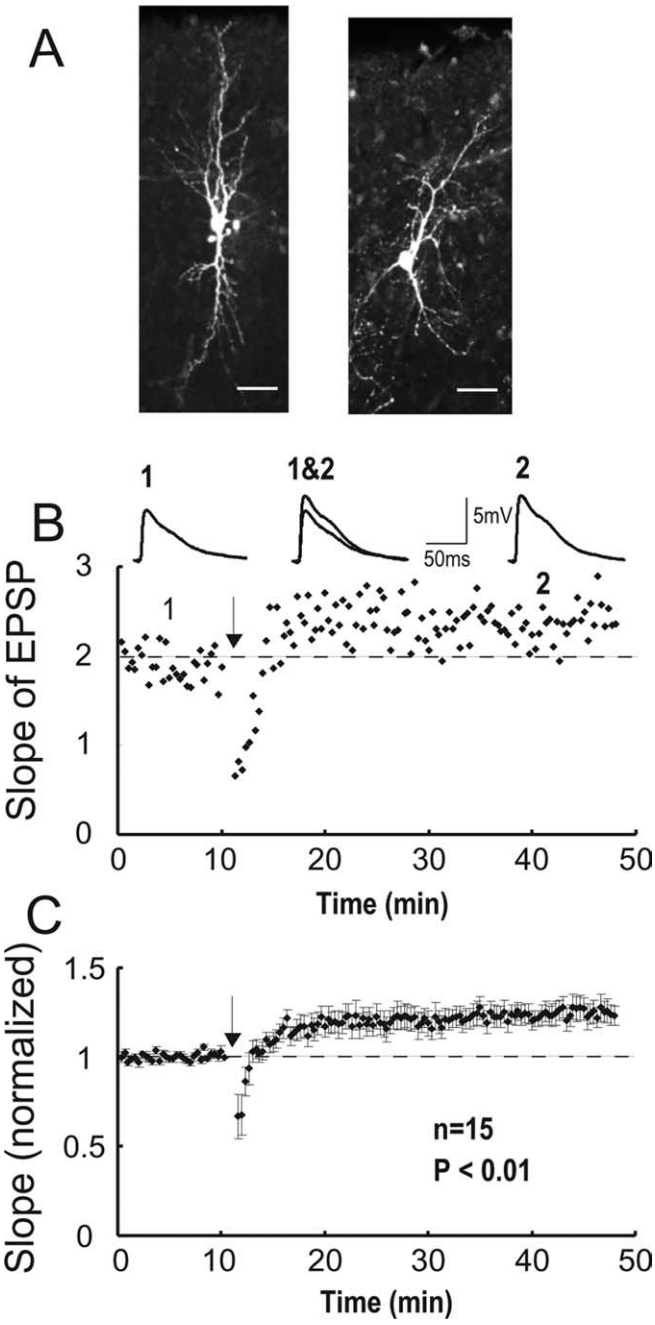

Figure 1. sSC LTP in narrow-field vertical neurons is induced by SO stimulation at 20 Hz for 20 s. ***A***, Confocal images of Texas Red staining for biocytin loaded in sSC narrow-field vertical neurons recorded in whole-cell mode. Scale bars, 40 μm. ***B***, Representative LTP induction with 20 Hz for 20 s stimulation in a single neuron. Data points represent the EPSP slope before and after induction (arrow). Traces represent averages of 30 responses obtained during 10 min of baseline (1) and 25–35 min after LTP induction (2). ***C***, Summary of all LTP experiments using the 20 Hz for 20 s induction stimulus. Data points represent mean EPSP slope (±SEM; $n = 15$). The mean EPSP slope ($t = 25$–35 min after induction) was significantly elevated to 124.3 ± 6.2% over the baseline value ($t = 0$–10 min).

Requirement of postsynaptic Ca^{2+} elevation in LTP induction

Postsynaptic Ca^{2+} transients are known to be critical for the induction of LTP at many synapses. The importance of postsynaptic Ca^{2+} flux to sSC LTP was examined by loading neurons with the fast Ca^{2+} buffer BAPTA (10 mM) from the recording pipette as soon as whole-cell configuration was attained. In the

presence of BAPTA, the 20 Hz, 20 s stimulating paradigm was totally ineffective at modifying SO-to-SGS synaptic strength. At 25–35 min after the inducing stimulation, the mean EPSP slope was 98.5 ± 3.5% of the control value ($n = 6$; $p = 0.13$) (Fig. 3*A*). Therefore, postsynaptic Ca^{2+} increases are required for the induction of LTP at SO-to-SGS excitatory synapses in the young rat SC.

Effects of blocking NMDARs and/or L-type Ca^{2+} channels on LTP induction

Previous reports have implicated NMDARs and/or L-type Ca^{2+} channels in LTP of the sSC field potentials (Okada, 1993; Platt and Withington, 1998; Lo and Mize, 2002). We therefore examined the effect of the competitive NMDAR antagonist AP-5 (50–100 μM) and the open L-type-Ca^{2+} channel blocker nimodipine (20 μM) on the induction of LTP. In the presence of bath-applied AP-5 or nimodipine alone, the LTP induction protocol (20 Hz, 20 s) failed to induce synaptic potentiation. Instead, it resulted in small depressions of the mean EPSP slopes to 92.8 ± 4.3% ($n = 17$; $p = 0.04$) for AP-5 (Fig. 3*B*) or to 82.5 ± 4.4% ($n = 21$; $p < 0.01$) for nimodipine (Fig. 3*C*). The increasing LTD after nimodipine (Fig. 3*C*) could be attributable to the fact that nimodipine is an open L-type Ca^{2+} channel blocker. Simultaneous bath application of both AP-5 and nimodipine abolished the LTP and did not induce LTD (100.2 ± 5.6%; $n = 8$; $p = 0.13$) (Fig. 3*D*). To control for an effect of 0.02% DMSO, in the nimodipine solvent, the 20 Hz for 20 s stimulation was applied with 0.02% DMSO alone and still elicited an increase in mean EPSP slope (120.6 ± 5.9%; $n = 6$; $p < 0.01$) (data not shown). This result was not significantly different from that observed in the normal LTP induction in Figure 1*C* ($p = 0.35$). Neither the application of AP-5, nimodipine, and 0.02% DMSO nor AP-5 plus nimodipine affected basal transmission. Thus, LTP induction at SO-to-SGS synapses requires postsynaptic Ca^{2+} elevation through both the NMDARs and L-type Ca^{2+} channels. Figure 3*E* displays the distribution of EPSP slope change in individual neurons 25–35 min after induction under different treatment conditions. The significance levels shown are those testing slope changes before and after LTP induction within each treatment using a paired *t* test. These data indicate an LTD with either nimodipine or AP-5 alone, but there is considerable variability in these responses across different neurons for the same treatment and across treatments. Because we could not assume equal variances, we therefore used the nonparametric Kruskal–Wallis test that showed a significant difference across treatments ($p \ll 0.001$), followed by the Steel–Dwass nonparametric *post hoc* test for pairwise comparisons between treatments. These tests revealed significant differences between normal 20 Hz, 20 s stimulation (no drug treatment) and AP-5 or nimodipine treatments, $p \ll 0.001$ and $p = 0.001$, respectively, and also differences between DMSO and AP-5 ($p = 0.009$), nimodipine ($p = 0.003$), or AP-5 plus nimodipine ($p = 0.043$). However, there was no strong evidence for differences between the AP-5 and the nimodipine treatments ($p = 0.52$), suggesting, as with the within-treatment *t* tests, that both these treatments cause an LTD. NMDAR and L-type Ca^{2+} channel activation was important for induction, not maintenance, of this sSC LTP because the LTP was not affected by washout of AP-5 or nimodipine after induction.

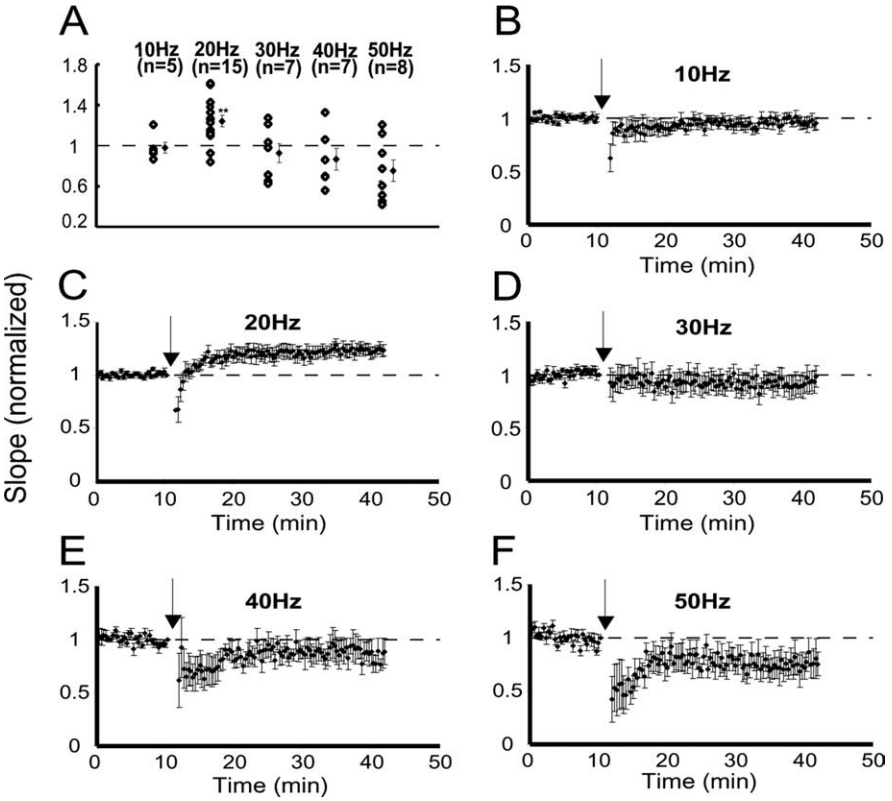

Figure 2. Stimulating current pulses at 20 Hz for 20 s produce the most reliable sSC LTP. Higher frequencies generally produce larger postinduction transient response depression as well as LTD. ***A***, Summary of EPSP slope changes 25–35 min after induction application at frequencies from 10 to 50 Hz. Each open diamond represents an individual experiment, whereas filled diamonds represent the mean of all experiments. Numbers in parentheses for this and all subsequent figures represents the number of experiments. ***B–F***, Summaries of slope changes before and after stimulation at 10, 20, 30, 40, and 50 Hz. With the exception of 30 Hz (***D***), increasing stimulus frequency caused a longer poststimulation depression, suggesting that the young synapses fail to follow prolonged and/or rapid pulses.

Substitution of Sr^{2+} for Ca^{2+} induces asynchronous quantal release

Substitution of Sr^{2+} for Ca^{2+} in the bath solution has frequently been used to determine whether synaptic plasticity involves changes in the size or the frequency of quantal events. However, in a system never before examined at this level it was important to determine that Sr^{2+} substitution indeed produced events identical to spontaneous miniature currents in the same neurons. Therefore, we examined the effect of substituting Sr^{2+} for Ca^{2+} (3 mM) on synaptic transmission at SO-to-SGS synapses.

Stimulation of SO, while holding cells at −70 mV in the presence of Ca^{2+}, produced fast synchronous EPSCs with no long-latency responses. Substituting Ca^{2+} with Sr^{2+} (3 mM) led to a decrease in the amplitude of synchronous EPSCs and to the appearance of asynchronous synaptic events (Fig. 4*A*). Sr^{2+}-induced asynchronous synaptic responses (Fig. 4*Ba*) were completely blocked by TTX (Fig. 4*Bb*), indicating that asynchronous synaptic responses observed in the presence of Sr^{2+} are initiated by afferent activation. In the same neuron, miniature EPSCs (mEPSCs) were recorded 10 min after slices were washed with

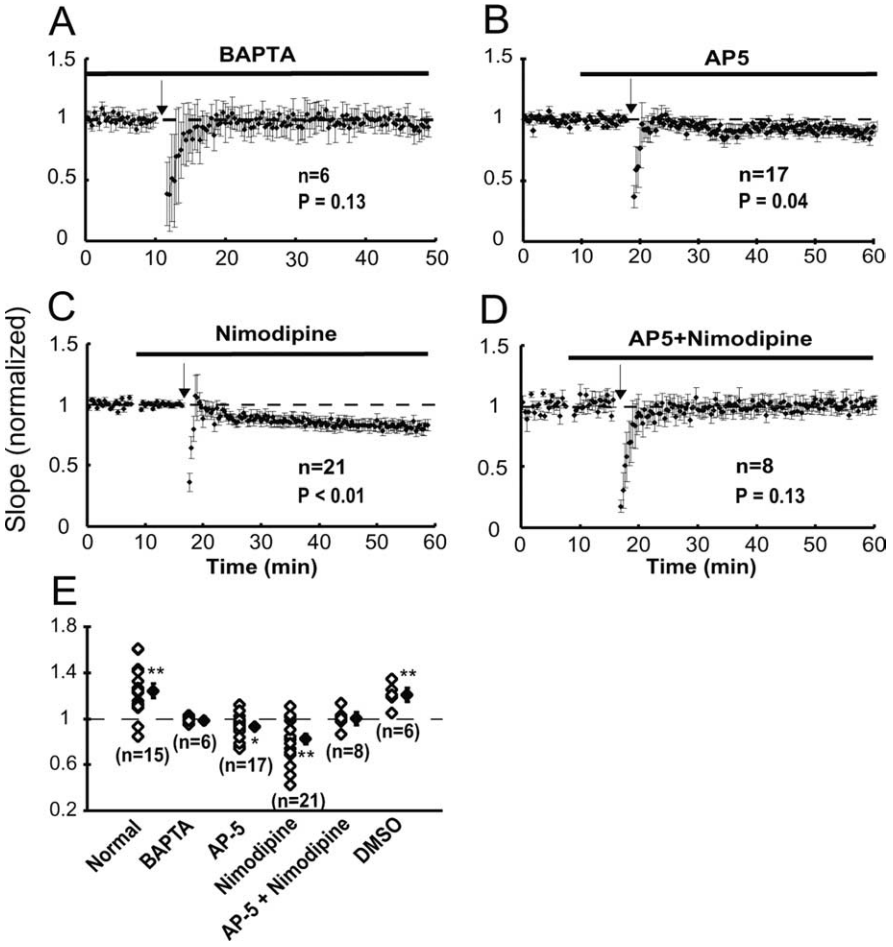

Figure 3. sSC LTP requires elevation of postsynaptic Ca^{2+} and depends on simultaneous activation of NMDARs and L-type Ca^{2+} channels. ***A***, A summary of all experiments in which BAPTA (10 mM) was included in the whole-cell patch pipette. This postsynaptic BAPTA prevented the induction of LTP. Data points represent mean EPSP slope (±SEM; $n = 7$). The mean EPSP slope (t = 25–35 min after induction) was not changed significantly over the baseline (t = 0–10 min). ***B***, ***C***, Application of AP-5 (50–100 μM; ***B***) or nimodipine (20 μM; ***C***) during induction prevents LTP and also produces a small LTD. ***D***, Application of both AP-5 and nimodipine blocks LTP. ***E***, Summary of mean EPSP slope changes at 25–35 min relative to baseline values after stimulation under the different perfusion conditions (notation as in Fig. 2). Analyses across treatments using Kruskal–Wallis and Steel–Dwass multiple comparison procedures did not detect significant differences among results for AP-5, nimodipine, and AP-5 plus nimodipine. DMSO is a control. DMSO was used as a solvent for solutions containing nimodipine.

duction of LTP can wash out quickly (~15 min) with whole-cell recording (Malinow and Tsien, 1990), sequential application of Sr^{2+} and recording of Sr^{2+}-induced asynchronous responses before and after LTP induction was not feasible (Oliet et al., 1996). Thus, perforated patch-clamp recording was used in the subsequent experiments. Slices were first superfused with Sr^{2+}–ACSF to produce asynchronous events under voltage-clamp configuration (Fig. 5*A*) and then washed with Ca^{2+}–ACSF under current-clamp configuration. After the EPSP amplitude stabilized (5–10 min), LTP was induced (Fig. 5*B*). After LTP remained stable for at least 35 min, both Sr^{2+}–ACSF perfusion and voltage-clamp recording configuration were reapplied. Once evoked, synchronous EPSC amplitude reached a steady level in the presence of Sr^{2+} (5–10 min), and asynchronous events were acquired as above. Figure 5, *B* and *C*, illustrates LTP like that in Figure 1, *B* and *C*; the mean EPSP slope 25–35 min after LTP induction was increased to 124.7 ± 7.3% over the baseline value ($n = 8$; $p < 0.01$). Comparison of the cumulative probabilities of amplitude for the asynchronous synaptic responses before and after LTP induction revealed no significant difference ($n = 8$; $p = 0.89$) (Fig. 5*D*). However, comparison of the cumulative probabilities of asynchronous synaptic event intervals showed that the intervals were significantly shortened after versus before LTP induction ($n = 8$; $p < 0.01$) (Fig. 5*E*). This increase in frequency of quantal events could result from an increase in the probability of presynaptic transmitter release, or it could reflect an increase in the number of functional synapses via postsynaptic increases in AMPARs at PSDs.

Ca^{2+} (3 mM)–ACSF in the presence of TTX (Fig. 4*Bc*). The mEPSCs disappeared after application of bath DNQX (10 μM), as expected at −70 mV in Mg^{2+}-containing ACSF (Fig. 4*Bd*). When the cumulative amplitude distribution of Sr^{2+}-induced asynchronous synaptic events were compared with that of mEPSCs recorded in the same neuron in the presence of TTX and Ca^{2+}, the amplitude distribution of Sr^{2+}-induced asynchronous responses were indistinguishable from those of mEPSCs in three neurons examined ($n = 3$; $p = 0.49$) (Fig. 4*C*). Consistent with previous observations (Oliet et al., 1996; Choi and Lovinger, 1997), these data indicate that Sr^{2+}-induced asynchronous synaptic responses at SO-to-SGS synapses in the rat sSC are quantal.

Association of LTP with increases in quantal frequency, but not quantal amplitude

LTP in CA1 has been found to change both frequency and amplitude of quantal events (Oliet et al., 1996). To determine the responses of quantal events at SO-to-SGS synapses after LTP, we compared both amplitude and frequency of asynchronous synaptic responses before and after LTP induction. Because the in-

No change in PPR and CV after LTP induction

To determine whether presynaptic release probability increased with sSC LTP, we calculated PPR and CVs before and after LTP induction (Fig. 6). Pairs of stimuli with 50 ms interstimulus intervals were delivered to cells held at −70 mV before and after inducing LTP. Similar to before, LTP was induced in current clamp. Typical paired-pulse recordings of the test stimuli are shown in the traces of Figure 6*A*. Graphs separately reflecting the potentiation of the first EPSC1 and the second EPSC2 in this experiment are shown below the traces, along with the PPR calculated for each test recording (Fig. 6*B*). The average potentiation across all five neurons examined with this protocol for the first test EPSC1 is shown in Figure 6*C*, and the PPR for each of the five neurons before and after LTP is illustrated in Figure 6*D*. These data indicate that the PPR does not change at afferent synapses onto narrow-field vertical neurons after LTP induction (before LTP, 1.0 ± 0.18; after LTP, 0.99 ± 0.17; $n = 5$; $p = 0.45$). The CV of EPSC1 amplitudes before and after LTP induction was also calculated for all five neurons (Fig. 6*E*). The CVs were also

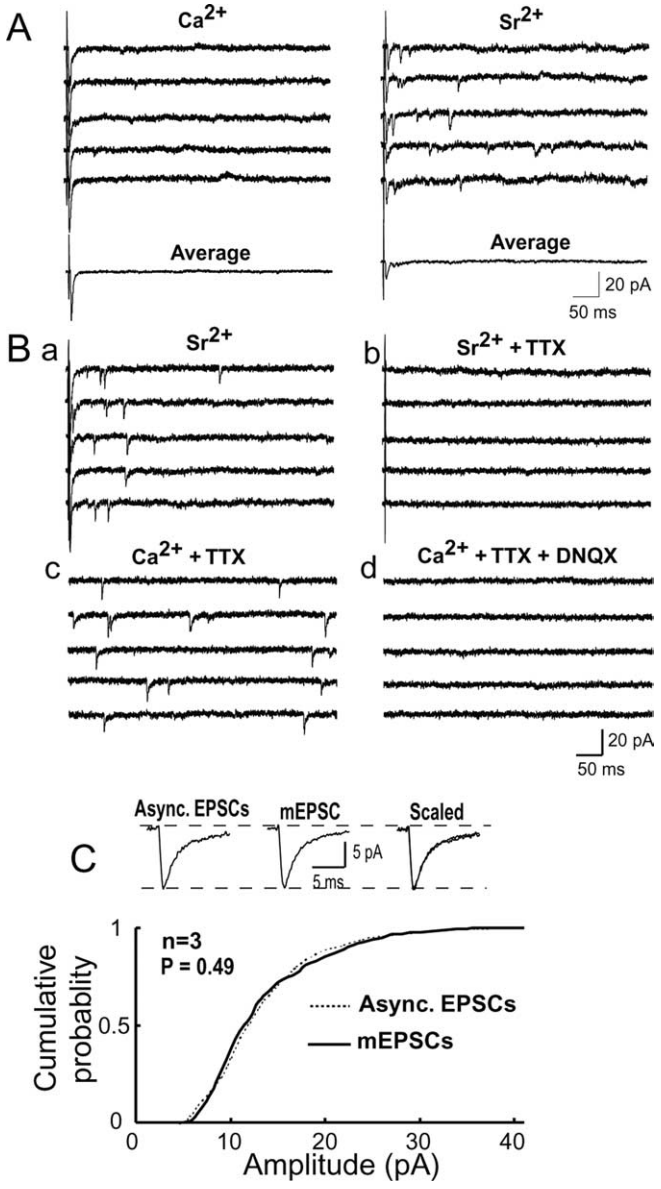

Figure 4. Substituting Sr^{2+} for Ca^{2+} induces asynchronous quantal synaptic release in neurons held at −70 mV with normal Mg^{2+} (3 mM) in the perfusion solution. ***A***, Sample traces of evoked EPSCs obtained in a narrow-field vertical neuron held at −70 mV in normal Mg^{2+}–ACSF with either Ca^{2+} or Sr^{2+}. Small asynchronous synaptic responses appear in the presence of Sr^{2+}. The bottom two traces are averages of 10 EPSCs showing that the synchronous synaptic responses are decreased in the presence of Sr^{2+}. ***B***, Sample traces recorded sequentially from the same neuron showing that asynchronous responses are driven by presynaptic stimulation and spontaneous mEPSCs are glutamatergic. Synchronous and asynchronous EPSCs evoked in the presence of Sr^{2+} (***Ba***) disappear after adding TTX (***Bb***). Spontaneous mEPSCs in the presence of Ca^{2+} and TTX (***Bc***) are blocked by adding DNQX (***Bd***). Notice that spontaneous mEPSCs are higher in frequency in (***Bc***) than in the period after the evoked current in ***A***. This probably reflects a relatively long vesicle recycling time (Ryan and Smith, 1995) after evoked release. ***C***, Cumulative amplitude distributions comparing evoked asynchronous EPSCs (Async. EPSCs) in the presence of Sr^{2+} (dotted line) with spontaneous mEPSCs in the presence of Ca^{2+} and TTX (solid line). The distribution represents averaged data from three neurons studied with the sequence in ***B***. The traces are averages of 40–50 evoked asynchronous EPSCs and 40–50 spontaneous mEPSCs recorded from the neuron shown in ***B***.

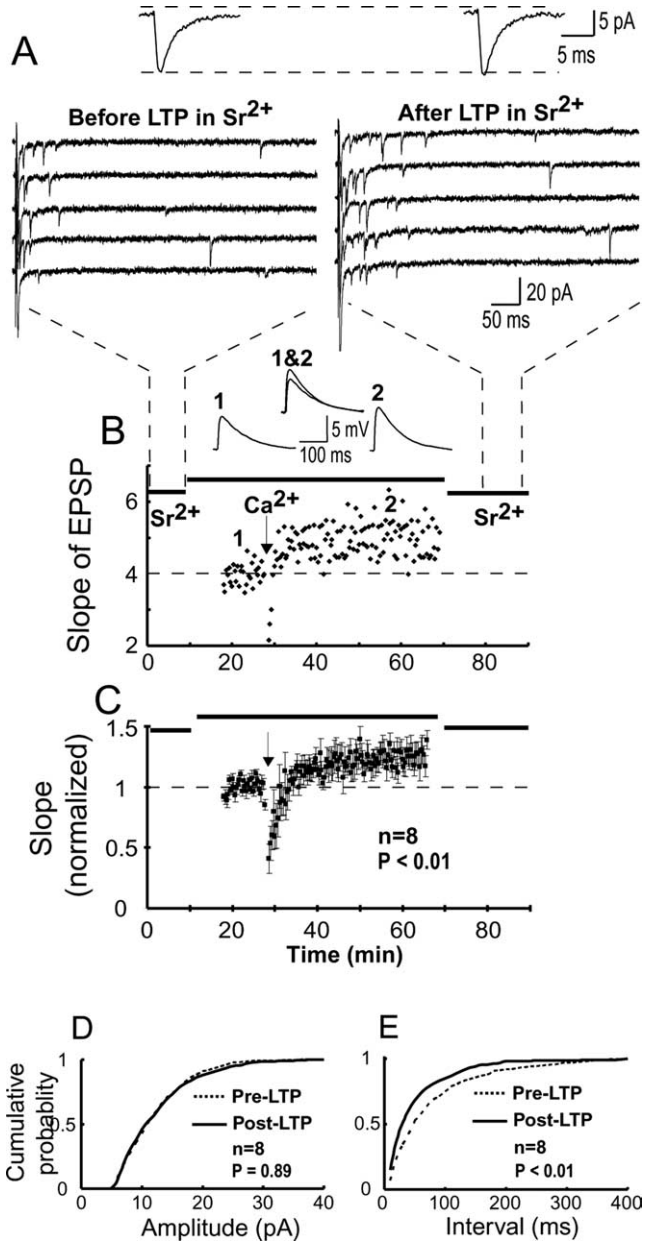

Figure 5. LTP expression is associated with an increase in quantal event frequency but not with a change in quantal amplitude. ***A***, Sample traces of evoked EPSCs obtained from a narrow-field vertical neuron in the presence of Sr^{2+} before and after induction of LTP. Averages of evoked asynchronous quantal events recorded sequentially before and after LTP induction are displayed above the sample traces. ***B***, LTP induction in the same neuron during perfusion of Ca^{2+}–ACSF. Data points represent the EPSP slope before and after the stimulation at 20 Hz for 20 s (arrow). Averages (EPSP1 and EPSP2) of 30 traces obtained during the 10 min before and 25–35 min after LTP induction in the cell are displayed above. Numbers mark the intervals where the averages were taken. ***C***, Summary of all experiments using this protocol. Data points represent mean EPSP slope (±SEM; $n = 8$). The mean EPSP slope ($t = 25$–35 min after induction) was significantly increased over the baseline (10 min before induction). ***D***, ***E***, Cumulative amplitude (***D***) and interval (***E***) distributions of the Sr^{2+}-induced asynchronous events obtained before (Pre; dotted line) and after (Post; solid line) LTP induction ($n = 8$ neurons). The cumulative amplitude distributions show no significant difference, whereas the cumulative interval distributions display a statistically significant shortening after LTP.

not significantly changed after LTP induction (before LTP, 0.12 ± 0.007; after LTP, 0.13 ± 0.006; $n = 5$; $p = 0.37$). These data indicate that the increase in quantal frequency after LTP in the sSC was not because of an increase in the probability of release from the sSC afferents. Instead, the results suggest that NMDAR and L-type Ca^{2+} LTP expression in the sSC results from an increase in functional synaptic contacts onto the narrow-field vertical excitatory neurons of the sSC.

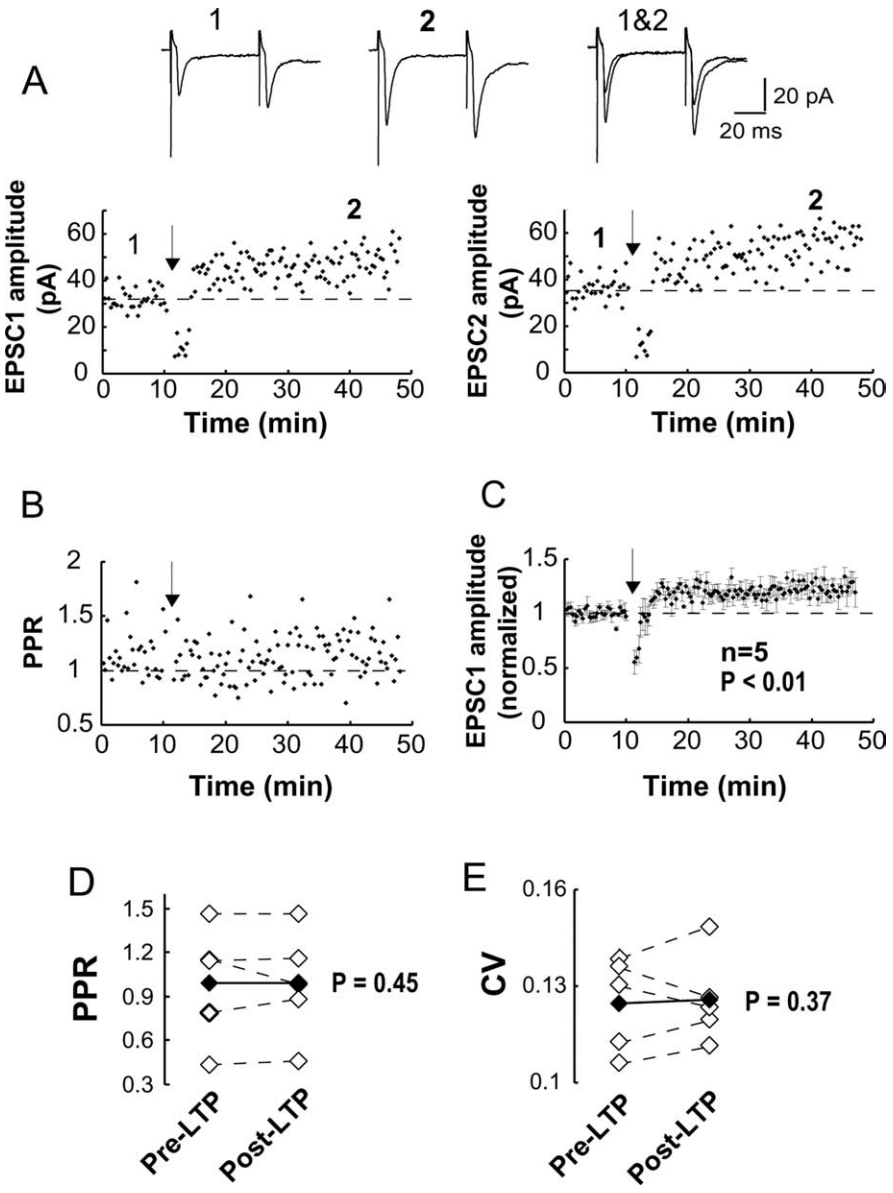

Figure 6. LTP expression occurs without changes in the probability of presynaptic release. ***A***, Traces of 30 average paired EPSC responses recorded at the time window indicated by the numbers before (1) and after (2) LTP induction. Examples of induction assayed as the peak amplitudes of EPSC1 (left) and of EPSC2 (right) plotted against time before and after LTP induction. ***B***, PPRs for the corresponding time points from the same cell. ***C***, Average of normalized EPSC1 peak amplitude from five experiments. Mean, normalized EPSC1 amplitude 25–35 min after tetanus was increased to 121.4 ± 6.8% over baseline value. ***D***, ***E***, Summaries of the PPRs and CVs from the same five experiments before (Pre) and after (Post) LTP induction. Means of PPRs and CVs from each individual experiment are indicated by open diamonds. Means of data averaged over all experiments either before or after LTP are indicated by closed circles. There are no significant differences between PPR or CV before compared with after LTP induction.

Discussion

In this study, we show that electrical stimulation *in vitro* induces LTP of SO-to-SGS synapses onto the excitatory narrow-field vertical neurons of the sSC (Langer and Lund, 1974; Mooney et al., 1985). This LTP requires postsynaptic Ca^{2+} elevation by NMDARs and L-type Ca^{2+} channels during induction but not maintenance. During LTP at hippocampal CA3-to-CA1 synapses, activation of L-type Ca^{2+} channels can increase the potentiation produced by NMDARs, but they are not necessary for its production (Grover and Teyler, 1990; Cavus and Teyler, 1996). In contrast, consistent with previous field potential studies of sSC LTP (Lo and Mize, 2000, 2002), the current work demonstrates that simultaneous function of L-type Ca^{2+} channels and NMDARs are essential for induction of LTP.

The stimulation regimen necessary to induce reliable single-cell SO-to-SGS LTP was 20 Hz for 20 s. This stimulation frequency is lower than stimuli generally used to generate LTP in CA1 neurons, although 25 Hz stimuli have been shown to produce a reliable LTP in these cells (Cavus and Teyler, 1996). Using an isolated brainstem preparation, Lo and Mize (2002) were able to induce LTP with the 50 Hz for 20 s regimen. In our single-cell slice recordings, we find that SO stimulation at 50 Hz for 20 s actually depresses the response. The difference could be as a result of field potential versus single-cell recording or whole-mounted brainstem versus slice recording, because more afferent axons may be activated in the former situation, which perhaps masks fatigue in a proportion of the afferents.

Variable forms of LTP in the mammalian sSC

Although NMDAR-dependent LTP has been studied in the optic tectum of fish (Schmidt, 1990) and in the semi-intact larval *Xenopus* tectum (Zhang et al., 1998, 2000), the results of previous studies of LTP in the SC of rodents have not focused on single-cell responses and have reported a variety of procedures that either produce or block sSC LTP. As cited above, Lo and Mize (2000, 2002) obtained results similar to ours, although most of their recordings were from younger or from older animals. Miyamoto et al. (1990) suggested that sSC field potential LTP induced by stimulation of the optic layer was not blocked by NMDAR antagonists but rather masked because washout of D-APV showed an established LTP without subsequent induction. However, Miyamoto and Okada (1993) used optic tract stimulation to show that induction of sSC field potential LTP was dependent on NMDARs. Platt and Withington (1998) used GABA application to SC slices to induce a field potential LTP that was independent of $GABA_A$ and $GABA_B$ receptors. This unusual role of GABA in potentiating sSC responses may be attributable to disinhibition by $GABA_C$ receptors, because $GABA_C$ receptors are now known to play a significant role in sSC disinhibition (Schmidt et al., 2001). Using intact rats, Hirai and Okada (1993) reported that the LTP in the superficial layers of the sSC was inhibited by visual cortical input. The inhibition was eliminated by picrotoxin or cortical removal. The result is not unexpected, because in the mature visual system many cortical inputs suppress sSC activity (Berman and Sterling, 1976) by providing large excitatory input to SC GABAergic neurons (Mize, 1992). Glycine addition to SC slices also induces sSC field potential LTP, and the effect is not blocked by strychnine or

APV but is eliminated by the L-type Ca^{2+} channel antagonist nifedipine (Platt et al., 1998). Although this result is consistent with the requirement for L-type Ca^{2+} channel activity in sSC LTP, mechanisms of interaction between glycine and L-type Ca^{2+} channels remain unknown. These diverse reports about sSC LTP and a need for data concerning single-cell responses motivated our work.

Cellular changes underlying LTP

When compared with CA3-to-CA1 LTP, our sSC LTP differs in specific qualitative respects. First, the narrow 20 Hz frequency dependence of SO-to-sSC LTP induction (Fig. 2*A*) is unlike that seen in CA3-to-CA1 LTP in which inducing frequencies range from ~25 to 200 Hz (Grover and Teyler, 1990; Moosmang et al., 2005). The narrow frequency range for induction in the sSC is likely to be attributable to a combination of parameters. For example, one factor is likely to be an inability of afferents to follow high frequencies. Our stimuli were delivered to the SO, where they drove both the established retinal afferents and the immature corticocollicular synapses. The corticocollicular projection only begins dense, localized arborization in the colliculus as a result of eye opening around P14 (Inoue et al., 1992; Goldberg and Constantine-Paton, 2005). Thus, immature corticocollicular synapses may be more likely than the CA3 afferents to exhaust transmitter in response to high-frequency stimuli because of smaller releasable pools of vesicles. This possibility is supported by our observation that, along with the progressive decrease in ability to induce LTP and a tendency to induce LTD as the frequency of stimulation is increased (Fig. 2*A*), the transient depression seen after 20 Hz stimulation (Figs. 1*C*, 5*C*, 6*C*) becomes more prolonged with higher-frequency stimulation (Fig. 2*C*,*E*,*F*). An alternative, but not mutually exclusive, possibility is that the narrow-field vertical neurons examined in the sSC may have a more prolonged AMPAR desensitization (Sun et al., 2002) than CA1 pyramids.

A second qualitative difference between LTP in the hippocampus and the sSC is that LTP onset in the sSC consistently lacks the short post-tetanic potentiation seen standardly at the CA3-to-CA1 synapse. Possibly the depression after inducing stimulation masks short-term potentiation that would otherwise result from residual Ca^{2+} in the SO terminals. Afferent sSC terminals might also lack post-tetanic potentiation for reasons relating to their morphology and consequent Ca^{2+} retention (Zucker and Regehr, 2002).

Silent synapses, LTP, and opportunities for synapse refinement

A final significant difference between CA3-to-CA1 and SO-to-narrow-field sSC neuron LTP arises from the Sr^{2+} analyses of evoked quantal events at both synapses. Unlike the CA1 synapses studied (Oliet et al., 1996), electrically induced sSC LTP does not produce a change in quantal amplitude; only an increase in mEPSCs frequency is observed. This frequency increase does not reflect a change in the probability of transmitter release because neither the PPR nor the CV of the EPSCs differed after compared with before LTP. Thus, LTP at these sSC synapses appears to reflect an increase in the number of synapses with functional AMPARs without any addition of AMPARs to pre-existing synapses. In hippocampus CA1, both amplitude and frequency of miniature EPSPs change with NMDAR-dependent LTP, and increases in miniature current frequency likely arise from increased probability of vesicle release and from AMPAR addition to otherwise NMDAR only "silent" synapses (Bekkers and Stevens, 1990; Malinow and Tsien, 1990; Liao et al., 1995; Isaac et al., 1996, 1997; Oliet et al., 1996).

Silent synapses are particularly prevalent in young tissue and are the first glutamatergic contacts present (Durand et al., 1996; Wu et al., 1996; Isaac et al., 1997; Rumpel et al., 1998). In the sSC, the glutamate-mediated currents appear near the end of the first postnatal week and contain few AMPAR currents (Shi et al., 2000). However, a large second increase in silent synapses occurs more than 1 week later after eye opening. After eye opening, silent synapse increases appear before and then overlap with a significant increase in both frequency and amplitude of quantal AMPAR events (Lu and Constantine-Paton, 2004). Slices in the current experiments were from animals 2–4 d after eye opening and therefore contained a large number of silent synapses. Such contacts can rapidly incorporate or stabilize AMPAR receptors in response to postsynaptic depolarization during stimulation (Liao et al., 1995; Isaac et al., 1997). Our data suggested that increases in the number of AMPARs at pre-existing synapses are less likely to occur when many synapses have no AMPARs (e.g., when the density of silent synapses is high).

Conclusion

A long-lasting increase in AMPAR-evoked responses has recently been generated in specific neurons of rodent prefrontal cortex by overexpressing the NMDAR and AMPAR PSD scaffold protein PSD-95. In this preparation, as in our experiments, the AMPAR increases were associated with an increase in miniature AMPAR current frequency and no change in quantal amplitude (Beique and Andrade, 2003). The second wave of silent synapses in sSC neurons shortly after eye opening is tightly associated with a rapid increase in PSD-95 in visual neuron dendrites and synapse (Yoshii et al., 2003) as well as synaptic rearrangement (Lu and Constantine-Paton, 2004). Perhaps normal developmental increases in PSD-95, before stabilizing more AMPARs at preexisting contacts, actually facilitate the development of new functional contacts by holding AMPARs at all contacts that happen to release glutamate onto "extrasynaptic" NMDARs when any depolarization allows Ca^{2+} into the postsynaptic process. Electrical stimulation would synchronously unsilence such contacts. However, the normal stochastic process could produce many new labile but, nevertheless, functional contacts and provide increased opportunity for activity-dependent sorting based on the patterns of correlated and uncorrelated activity among the afferents that converge on the cell by trial and error. Such a mechanism would greatly facilitate the rate of activity-dependent refinement of connections in the developing brain.

References

Beique JC, Andrade R (2003) PSD-95 regulates synaptic transmission and plasticity in rat cerebral cortex. J Physiol (Lond) 546:859–867.

Bekkers JM, Stevens CF (1990) Presynaptic mechanism for long-term potentiation in the hippocampus. Nature 346:724–729.

Berman N, Sterling P (1976) Cortical suppression of the retino-collicular pathway in the monocularly deprived cat. J Physiol (Lond) 255:263–273.

Cavus I, Teyler T (1996) Two forms of long-term potentiation in area CA1 activate different signal transduction cascades. J Neurophysiol 76:3038–3047.

Choi S, Lovinger DM (1997) Decreased frequency but not amplitude of quantal synaptic responses associated with expression of corticostriatal long-term depression. J Neurosci 17:8613–8620.

Constantine-Paton M (1990) NMDA receptor as a mediator of activity-dependent synaptogenesis in the developing brain. Cold Spring Harb Symp Quant Biol 55:431–443.

Constantine-Paton M, Cline HT (1998) LTP and activity-dependent synaptogenesis: the more alike they are, the more different they become. Curr Opin Neurobiol 8:139–148.

Colonnese MT, Zhao JP, Constantine-Paton M (2005) NMDA receptor currents suppress synapse formation on sprouting axons *in vivo*. J Neurosci 25:1291–1303.

Dalva MB, Takasu MA, Lin MZ, Shamah SM, Hu L, Gale NW, Greenberg ME (2000) EphB receptors interact with NMDA receptors and regulate excitatory synapse formation. Cell 103:945–956.

Durand GM, Kovalchuk Y, Konnerth A (1996) Long-term potentiation and functional synapse induction in developing hippocampus. Nature 381:71–75.

Goldberg JR, Constantine-Paton M (2005) Eye-opening dependent elaboration and refinement of the corticocollicular visual pathway. Soc Neurosci Abstr 31:714.15.

Groc L, Gustafsson B, Hanse E (2006) AMPA signalling in nascent glutamatergic synapses: there and not there! Trends Neurosci 29:132–139.

Grover LM, Teyler TJ (1990) Two components of long-term potentiation induced by different patterns of afferent activation. Nature 347:477–479.

Hirai H, Okada Y (1993) Ipsilateral corticotectal pathway inhibits the formation of long-term potentiation (LTP) in the rat superior colliculus through GABAergic mechanism. Brain Res 629:23–30.

Hughes DI, Bannister AP, Pawelzik H, Thomson AM (2000) Double immuno fluorescence, peroxidase labelling and ultrastructural analysis of interneurones following prolonged electrophysiological recordings *in vitro*. J Neurosci Methods 101:107–116.

Inoue K, Terashima T, Inoue Y (1992) Postnatal development of the corticotectal projection from the visual cortex of the mouse. Okajimas Folia Anat Jpn 68:319–331.

Isaac JT, Oliet SH, Hjelmstad GO, Nicoll RA, Malenka RC (1996) Expression mechanisms of long-term potentiation in the hippocampus. J Physiol (Paris) 90:299–303.

Isaac JT, Crair MC, Nicoll RA, Malenka RC (1997) Silent synapses during development of thalamocortical inputs. Neuron 18:269–280.

Jeon CJ, Gurski MR, Mize RR (1997) Glutamate containing neurons in the cat superior colliculus revealed by immunocytochemistry. Vis Neurosci 14:387–393.

Langer TP, Lund RD (1974) The upper layers of the superior colliculus of the rat: a Golgi study. J Comp Neurol 158:418–435.

Liao D, Hessler NA, Malinow R (1995) Activation of postsynaptically silent synapses during paring-induced LTP in CA1 region of hippocampal slice. Neuron 375:400–404.

Lo FS, Mize RR (2000) Synaptic regulation of L-type Ca^{2+} channel activity and long-term depression during refinement of the retino collicular pathway in developing rodent superior colliculus. J Neurosci 20:RC58(1–6).

Lo FS, Mize RR (2002) Properties of LTD and LTP of retinocollicular synaptic transmission in the developing rat superior colliculus. Eur J Neurosci 5:1421–1432.

Lu W, Constantine-Paton M (2004) Eye opening rapidly induces synaptic potentiation and refinement. Neuron 43:237–249.

Magee JC (2000) Dendritic integration of excitatory synaptic input. Nat Rev Neurosci 1:181–190.

Malinow R, Tsien RW (1990) Presynaptic enhancement shown by whole-cell recordings of long-term potentiation in hippocampal slices. Nature 346:177–180.

McLaughlin T, O'Leary DD (2005) Molecular gradients and development of retinotopic maps. Annu Rev Neurosci 28:327–355.

Miyamoto T, Okada Y (1993) NMDA receptor, protein kinase C and calmodulin system participate in the long-term potentiation in guinea pig superior colliculus slices. Brain Res 605:287–292.

Miyamoto T, Sakurai T, Okada Y (1990) Masking effect of NMDA receptor antagonists on the formation of long-term potentiation (LTP) in superior colliculus slices from the guinea pig. Brain Res 518:166–172.

Mize RR (1992) The organization of GABAergic neurons in the mammalian superior colliculus. Prog Brain Res 90:219–248.

Mize RR, Graham SK, Cork RJ (2002) Expression of the L-type calcium channel in the developing mouse visual system by use of immunocytochemistry. Brain Res Dev Brain Res 136:185–195.

Mooney RD, Klein BG, Rhoades RW (1985) Correlations between the structural and functional characteristics of neurons in the superficial laminae and the hamster's superior colliculus. J Neurosci 5:2989–3009.

Moosmang S, Haider N, Klugbauer N, Adelsberger H, Langwieser N, Müller J, Stiess M, Marais E, Schulla V, Lacinova L, Goebbels S, Nave KA, Storm DR, Hofmann F, Kleppisch T (2005) Role of hippocampal Cav1.2 Ca^{2+} channels in NMDA receptor-independent synaptic plasticity and spatial memory. J Neurosci 25:9883–9892.

Nicoll RA (2003) Expression mechanisms underlying long-term potentiation: a postsynaptic view. Philos Trans R Soc Lond B Biol Sci 358:721–726.

Okada Y (1993) The properties of the long-term potentiation (LTP) in the superior colliculus. Prog Brain Res 95:287–296.

Oliet SH, Malenka RC, Nicoll RA (1996) Bidirectional control of quantal size by synaptic activity in the hippocampus. Science 271:1294–1297.

Platt B, Withington DJ (1998) GABA-induced long-term potentiation in the guinea-pig superior colliculus. Neuropharmacology 37:1111–1122.

Platt B, Bate JR, von Linstow Roloff E, Withington DJ (1998) Glycine induces a novel form of long-term potentiation in the superficial layers of the superior colliculus. Br J Pharmacol 125:293–300.

Poncer JC (2003) Hippocampal long term potentiation: silent synapses and beyond. J Physiol (Paris) 97:415–422.

Rumpel S, Hatt H, Gottmann K (1998) Silent synapses in the developing rat visual cortex: evidence for postsynaptic expression of synaptic plasticity. J Neurosci 18:8863–8874.

Ryan TF, Smith SJ (1995) Vesicle pool mobilization during action potential firing at hippocampal synapses. Neuron 14:983–989.

Schmidt JT (1990) Long-term potentiation and activity-dependent retinotopic sharpening in the regenerating retinotectal projection of goldfish: common sensitive period and sensitivity to NMDA blockers. J Neurosci 10:233–246.

Schmidt M, Boller M, Ozen G, Hall WC (2001) Disinhibition in rat superior colliculus mediated by $GABA_C$ receptors. J Neurosci 21:691–699.

Shi J, Townsend M, Constantine-Paton M (2000) Activity-dependent induction of tonic calcineurin activity mediates a rapid developmental downregulation of NMDA receptor currents. Neuron 28:103–114.

Simon DK, O'Leary DD (1992) Development of topographic order in the mammalian retinocollicular projection. J Neurosci 12:1212–1232.

Simon DK, Prusky GT, O'Leary DD, Constantine-Paton (1992) *N*-methyl-D-aspartate receptor antagonists disrupt the formation of a mammalian neural map. Proc Natl Acad Sci USA 89:10593–10597.

Sun Y, Olson R, Horning M, Armstrong N, Mayer M, Gouaux E (2002) Mechanism of glutamate receptor desensitization. Nature 417:245–253.

Torborg CL, Feller MB (2005) Spontaneous patterned retinal activity and the refinement of retinal projections. Prog Neurobiol 76:213–235.

Townsend M, Yoshii A, Mishina M, Constantine-Paton M (2003) Developmental loss of miniature N-methyl-D-aspartate receptor currents in NR2A knockout mice. Proc Natl Acad Sci USA 100:1340–1345.

van Zundert B, Yoshii A, Constantine-Paton M (2004) Receptor compartmentalization and trafficking at glutamate synapses: a developmental proposal. Trends Neurosci 27:428–437.

Wang Z, Xu NL, Wu CP, Duan S, Poo MM (2003) Bidirectional changes in spatial dendritic integration accompanying long-term synaptic modifications. Neuron 37:463–472.

Watanabe S, Hoffman DA, Migliore M, Johnston D (2002) Dendritic K+ channels contribute to spike-timing dependent long-term potentiation in hippocampal pyramidal neurons. Proc Natl Acad Sci USA 99:8366–8371.

Wu G, Malinow R, Cline HT (1996) Maturation of a central glutamatergic synapse. Science 274:972–976.

Yoshii A, Sheng MH, Constantine-Paton M (2003) Eye opening induces a rapid dendritic localization of PSD-95 in central visual neurons. Proc Natl Acad Sci USA 100:1334–1339.

Zhang LI, Tao HW, Holt CE, Harris WA, Poo M (1998) A critical window for cooperation and competition among developing retinotectal synapses. Nature 395:37–44.

Zhang LI, Tao HW, Poo M (2000) Visual input induces long-term potentiation of developing retinotectal synapses. Nat Neurosci 3:708–715.

Zucker RS, Regehr WG (2002) Short-term synaptic plasticity. Annu Rev Physiol 64:355–405.